

Do group dynamics play a role in the evolution of member galaxies?

Annie Hou,^{1*} Laura C. Parker,¹ Michael L. Balogh,² Sean L. McGee,^{3,4}
David J. Wilman,⁵ Jennifer L. Connelly,⁵ William E. Harris,¹ Angus Mok,²
John S. Mulchaey,⁶ Richard G. Bower³ and Alexis Finoguenov^{7,8}

¹Department of Physics & Astronomy, McMaster University, Hamilton, ON L8S 4M1, Canada

²Department of Physics and Astronomy, University of Waterloo, Waterloo, ON N2L 3G1, Canada

³Department of Physics, University of Durham, Durham DH1 3LE, UK

⁴Leiden Observatory, Leiden University, PO Box 9513, NL-2300 RA Leiden, the Netherlands

⁵Max-Planck-Institut für Extraterrestrische Physik, Giessenbachstraße, D-85748 Garching, Germany

⁶Observatories of the Carnegie Institution, 813 Santa Barbara Street, Pasadena, CA, USA

⁷Department of Physics, University of Helsinki, Gustaf Hallströmin katu 2a, FI-00014 Helsinki, Finland

⁸CSST, University of Maryland, Baltimore County, 1000 Hilltop Circle, Baltimore, MD 21250, USA

Accepted 2013 July 29. Received 2013 June 15; in original form 2013 April 3

ABSTRACT

We examine galaxy groups from the present epoch to $z \sim 1$ to explore the impact of group dynamics on galaxy evolution. We use group catalogues from the Sloan Digital Sky Survey (SDSS), the Group Environment and Evolution Collaboration (GEEC) and the high-redshift GEEC2 samples to study how the observed member properties depend on the galaxy stellar mass, group dynamical mass and dynamical state of the host group. We find a strong correlation between the fraction of non-star-forming (quiescent) galaxies and galaxy stellar mass, but do not detect a significant difference in the quiescent fraction with group dynamical mass, within our sample halo mass range of $\sim 10^{13} - 10^{14.5} M_{\odot}$, or with dynamical state. However, at $z \sim 0.4$ we do find some evidence that the quiescent fraction in low-mass galaxies [$\log_{10}(M_{\text{star}}/M_{\odot}) \lesssim 10.5$] is lower in groups with substructure. Additionally, our results show that the fraction of groups with non-Gaussian velocity distributions increases with redshift to $z \sim 0.4$, while the amount of detected substructure remains constant to $z \sim 1$. Based on these results, we conclude that for massive galaxies [$\log_{10}(M_{\text{star}}/M_{\odot}) \gtrsim 10.5$], evolution is most strongly correlated to the stellar mass of a galaxy with little or no additional effect related to either the group dynamical mass or the dynamical state. For low-mass galaxies, we do find some evidence of a correlation between the quiescent fraction and the amount of detected substructure, highlighting the need to probe further down the stellar mass function to elucidate the role of environment in galaxy evolution.

Key words: galaxies: formation – galaxies: groups: general – galaxies: kinematics and dynamics.

1 INTRODUCTION

A long-standing debate is whether the evolution of galaxies is governed primarily by internal processes (e.g. feedback) or those related to the external environment (e.g. stripping). The morphology–density relation seen in the cores of clusters (Oemler 1974; Dressler 1980) was one of the first observations to show that the environment may influence the properties of galaxies, where elliptical and S0 (early-type) galaxies were found preferentially in high-density regions and spiral and irregular (late-type) galaxies in low-density

regions. Since then, numerous correlations between galaxy properties and environment have been observed. For example, differences in the distributions of colours (Blanton et al. 2003; Baldry et al. 2006; Hou et al. 2009), the fraction of either star-forming or quiescent galaxies (Balogh et al. 2004; Kauffmann et al. 2004; Wilman et al. 2005a; Peng et al. 2010; McGee et al. 2011; Patel et al. 2011; Sobral et al. 2011; Muzzin et al. 2012), and the amount of observed dust (Kauffmann et al. 2004). Correlations between environment and galaxy properties appear to have been in place since at least $z \sim 1$, as the observed star formation rate (SFR)–density and specific SFR (SSFR = SFR/stellar mass)–density relations show variations with environment at this redshift (Cooper et al. 2008; Patel et al. 2011).

* E-mail: houa2@physics.mcmaster.ca

Although there have been numerous observations of correlations between environment and galaxy properties, where red and quiescent galaxies are preferentially found in higher density regions, recent studies have suggested that internal or secular processes, traced by the mass of the galaxy, may actually be the dominant factor in galaxy evolution. In particular, several studies have found that the properties of actively star forming galaxies only weakly depend on the environment (Balogh et al. 2004; Wilman et al. 2005a; Poggianti et al. 2008; Peng et al. 2010; Tyler et al. 2011). Similarly, Muzzin et al. (2012) found that although the environment does determine the fraction of galaxies that remain actively star forming, the stellar populations of both actively star forming and quiescent galaxies are most strongly correlated to the stellar mass of a galaxy.

The emerging picture appears to suggest that *both* internal and external processes contribute to the evolution of galaxies. Although observations have shown that stellar mass correlates well with environment, both in the local Universe (Hogg et al. 2003; Kauffmann et al. 2004; Blanton et al. 2005; Baldry et al. 2006) and at $z \sim 1$ (Bolzonella et al. 2010; Sobral et al. 2011), recent studies have claimed that the effects due to the environment can still be disentangled from transformation processes traced by galaxy stellar mass (Peng et al. 2010; Sobral et al. 2011; Muzzin et al. 2012). In an empirically driven picture of galaxy evolution, Peng et al. (2010) claimed that the evolution of low-mass galaxies [$\log_{10}(M_{\text{star}}/M_{\odot}) \lesssim 10.5$] is dominated by environmentally driven star formation quenching, whereas high-mass galaxy evolution [$\log_{10}(M_{\text{star}}/M_{\odot}) \gtrsim 10.5$] is governed by processes that are traced by galaxy stellar mass.

Galaxy groups are ideal for studies of the role of the environment in the evolution of galaxies. Not only are groups the most common environment in the local Universe (Geller & Huchra 1983; Eke et al. 2005), but it is also believed that as many as 40 per cent of galaxies, especially low-mass galaxies, that live in rich groups or clusters were pre-processed (i.e. had their star formation quenched) in haloes with $M_{\text{halo}} \gtrsim 10^{13} h^{-1} M_{\odot}$ before infall (McGee et al. 2009; De Lucia et al. 2012).

The pre-processing of galaxies in low-mass groups may be driven by galaxy–galaxy interactions and mergers. As a result of the relatively low velocity dispersion observed in groups, it has been shown that the rate of mergers is higher in the group environment with respect to both the field and the richer galaxy clusters (Barnes 1985; Zabludoff & Mulchaey 1998a; Brough et al. 2006; De Lucia et al. 2011). Interactions are thought to initially trigger an intense burst of star formation (Sanders et al. 1988; Elbaz & Cesarsky 2003; Cox et al. 2006; Teysier, Chapon & Bournaud 2010), which can use up the supply of cold gas and lead to the quenching of star formation, if no further gas accretes on to the galaxy. Thus, mergers and interactions can either enhance or quench star formation depending on the evolutionary stage at which the galaxy is observed. In addition, star formation quenching in galaxies may occur as a satellite falls into a larger dark matter halo due to processes such as strangulation (Larson, Tinsley & Caldwell 1980; Balogh, Navarro & Morris 2000; Kawata & Mulchaey 2008) and ram-pressure stripping (Gunn & Gott 1972; Abadi, Moore & Bower 1999). Thus, galaxy evolution appears to be related to the accretion history of the galaxy and with the number of interactions the galaxy has experienced. By looking for correlations between group dynamics and member properties, it is possible to probe the importance of accretion history and dynamical interactions on the evolution of galaxies.

In this paper, we study the dependence of galaxy evolution on galaxy stellar mass, group dynamical mass and group dynamics. The paper is structured as follows. In Section 2, we describe the data and

group catalogues, as well as discuss the methods for determining the stellar mass and SFR. In Section 3, we look for correlations of galaxy properties with galaxy stellar mass and group dynamical mass. In Section 4, we classify the dynamical state of our groups and compare the properties of galaxies in dynamically young and dynamically evolved systems. We discuss our results in Section 5 and finally present our conclusions in Section 6.

Throughout this paper, we assume a Λ cold dark matter (Λ CDM) cosmology with $\Omega_{\text{m},0} = 0.27$, $\Omega_{\Lambda,0} = 0.73$ and $H_0 = 71 \text{ km s}^{-1} \text{ Mpc}^{-1}$.

2 DATA

In order to investigate the role of group dynamics in galaxy evolution, we look at three highly complete group catalogues that span a redshift range of $0 \lesssim z \lesssim 1$. This allows us to probe not only how the properties of the member galaxies depend on the properties of the host group, but also how these correlations evolve with redshift. The low-redshift ($0 < z < 0.12$) group sample is from the Sloan Digital Sky Survey (SDSS), the intermediate-redshift ($0.15 < z < 0.55$) sample is from the Group Environment and Evolution Collaboration (GEEC) survey and the high-redshift ($0.8 < z < 1$) groups are from the GEEC2 survey (to be discussed in detail in Sections 2.1–2.3).

2.1 The SDSS group catalogue

Although there are many publicly available SDSS group catalogues (e.g. Berlind et al. 2006; Yang et al. 2007), we elect to use the groups defined in McGee et al. (2011), who applied a multistage approach to mimic both the observing conditions and the group-finding algorithm used to identify our intermediate-redshift GEEC groups (see Section 2.2). This selection allows for a better comparison of the group and galaxy properties by reducing possible effects introduced by differences in the spectroscopic completeness, limiting magnitude or in the group-finding algorithm. A full description of our SDSS group catalogue is given in McGee et al. (2011), but we give a brief summary here. Groups were identified using galaxies observed in the SDSS Data Release 6 (DR6), which contains over 790 000 spectra in an area of $\sim 7425 \text{ deg}^2$ (Adelman-McCarthy et al. 2008). In addition to the SDSS *ugriz* photometry, McGee et al. (2011) made use of the overlapping *GALEX* Medium Imaging Survey, which covered an area of $\sim 1000 \text{ deg}^2$ of SDSS (Martin et al. 2005; Morrissey et al. 2007). The inclusion of the near-ultraviolet (NUV) and far-ultraviolet (FUV) bands is important for better estimates of the SFR.

To reproduce the observing conditions and group-finding algorithm of the second Canadian Network for Observational Cosmology (CNOC2) Galaxy Redshift Survey (Yee et al. 2000), on which the GEEC group catalogue is based, McGee et al. (2011) applied the same absolute magnitude cut and then randomly removed half the remaining galaxies to match the spectroscopic completeness of the CNOC2 redshift survey (see Section 2.2). With this sample, McGee et al. (2011) calculated the local density around each galaxy by counting the number of galaxies within a cylinder of $0.33 h_{75}^{-1} \text{ Mpc}$ and a line-of-sight depth of $\pm 6.67 h_{75}^{-1} \text{ Mpc}$. Protogroups were then identified starting from galaxies with the highest local densities and taking all of the galaxies within the cylinder centred around the high-density galaxies as protogroup members. Next, all of the galaxies in each of the cylinders centred on the initial members were added and the process continued until no further galaxies could be added. Using these protogroups, a preliminary geometric centre, redshift, velocity dispersion (σ) and virial radius

(r_{200} : equation 2) were computed. Protogroup members were then added or removed iteratively if they fell within $1.5r_{200}$ and 3σ of the group centre. Once all of the protogroups were identified, McGee et al. (2011) then added all of the SDSS galaxies back into the sample and group membership was finalized with a methodology similar to that used to identify the GEEC groups (Carlberg et al. 2001; Wilman et al. 2005b).

2.2 The GEEC group catalogue

Our intermediate-redshift sample is the GEEC group catalogue, which contains ~ 200 groups in the range of $0.1 < z < 0.55$. The GEEC survey is based on a set of groups first identified in the CNOC2 redshift survey (Yee et al. 2000; Carlberg et al. 2001), which contained $\sim 4 \times 10^4$ galaxies in four patches totalling $\sim 1.5 \text{ deg}^2$. The original photometry was taken in the $UBVR_cI_c$ bands down to a limiting magnitude of $R_c = 23.0$ and spectra were obtained for more than 6000 galaxies with a completeness of 48 per cent at $R_c = 21.5$ (Yee et al. 2000).

The GEEC survey built on the CNOC2 survey by obtaining higher spectroscopic completeness to a fainter limiting magnitude with 78 per cent completeness at $R_c = 22$ for a subset of the groups (Wilman et al. 2005b; Connelly et al. 2012). The extensive follow-up spectroscopy was taken with LDSS2 (Wilman et al. 2005b) and IMACS (Connelly et al. 2012) on Magellan, as well as data from FORS2 on the Very Large Telescope (Connelly et al. 2012). Additionally, we have obtained multiwavelength data from the X-ray to the infrared observed with the following telescopes: *XMM-Newton* (Finoguenov et al. 2009), *Chandra X-ray Observatory* (Finoguenov et al. 2009), *GALEX* (McGee et al. 2011), *HST-ACS* (Wilman et al. 2009), *Spitzer-MIPS* (Tyler et al. 2011), *Spitzer-IRAC* (Wilman et al. 2008), INGRID on the William Herschel Telescope (Balogh et al. 2009) and SOFI on the New Technology Telescope (Balogh et al. 2007). In addition, improved optical imaging was obtained in the *ugrizBVRI* filters from the Canada–France–Hawaii Telescope’s Megacam and CFH12K imagers (Balogh et al. 2009).

Group membership was defined with the friends-of-friends (FoF) algorithm outlined in Wilman et al. (2005b). An analysis of mock catalogues has shown that the contamination rate is 2.5 per cent for galaxies within $0.5 h_{75}^{-1} \text{ Mpc}$ of the group centroid (McGee et al. 2008).

2.3 The GEEC2 group catalogue

The high-redshift sample contains a subset of groups identified in the GEEC2 survey. A detailed discussion of the GEEC2 survey is presented in Balogh et al. (2011) and Mok et al. (2013). The goal of the GEEC2 survey was to obtain high spectroscopic completeness for 20 galaxy groups in the redshift range of $0.8 < z < 1.0$ that were initially identified in the Cosmological Evolution Survey (Scoville et al. 2007) with extended X-ray emission (Finoguenov et al. 2007; George et al. 2011). The follow-up spectroscopic survey is being conducted with the GMOS spectrograph on the GEMINI telescope and thus far data have been collected for 11 of the 20 target groups with spectroscopic completeness between ~ 0.6 and 0.75 (Balogh et al. 2011) down to $r = 24.75$.

Balogh et al. (2011) assigned group membership based on a galaxy’s proximity to the measured X-ray centre. It should be noted that although the group centroid for GEEC2 is based on X-ray emission, rather than a luminosity-weighted centre (used in SDSS and GEEC), Connelly et al. (2012) found that the difference between these two definitions is typically small ($< 18 \text{ arcsec}$) and that group

membership and overall group properties did not change significantly with either centroid. For each group, the velocity dispersion (σ) was computed from all galaxies within 1.0 Mpc and 4000 km s^{-1} of the measured group X-ray centre. Next the rms projected radial position from the group centroid (R_{rms}) was computed and all galaxies with group-centric velocities $> C_z \sigma$ and radial position $> C_r R_{\text{rms}}$ were clipped, where the typical values for C_z and C_r were 2. Finally, σ and R_{rms} were re-computed and only galaxies with $z < 2.5\sigma_{1 \text{ Mpc}}$ and radial positions $< 2R_{\text{rms}}$ were defined as group members.

Ideally, all three group catalogues would be defined in the same way; however, an unbiased and highly complete spectroscopic survey at high redshifts is a difficult and expensive task. Including the GEEC2 groups allows us to probe the high-redshift Universe. Additionally, GEEC2 is one of the few high-redshift group catalogues with high spectroscopic completeness and more than five members per group, allowing for studies of group dynamics.

2.4 Spectral energy distribution fitting

In Table 1, we list the group catalogue, redshift range, number of groups used in this analysis and the available photometry for each sample. We see that each of the three group catalogues has multiwavelength data (Table 1), which were used to measure stellar masses and SFRs via spectral energy distribution (SED) template fitting. The same fitting procedure was carried out for all catalogues from all available photometric bands. A detailed discussion of the SED-fitting procedure is given in McGee et al. (2011) for the SDSS and GEEC catalogues and in Balogh et al. (2011) for the GEEC2 catalogue. The observed photometry was compared to a grid of SEDs constructed with the Bruzual & Charlot (2003) stellar population synthesis code for the SDSS and GEEC catalogues and the Bruzual (2007) model for GEEC2. A Chabrier initial mass function (IMF) was assumed for all three catalogues. In both McGee et al. (2011) and Balogh et al. (2011), the SED-fitting procedure followed that outlined in Salim et al. (2007), where a grid of models that uniformly sampled the allowed parameters of formation time, galaxy metallicity and a two-component dust model (Charlot & Fall 2000) was created. An exponentially declining base SFR, with added bursts of star formation with varying duration and relative strength, was used to model the star formation history of each galaxy. Probability distribution functions were created for the relevant galaxy parameters after weighing each model by its $\exp(-\chi^2/2)$ and the median value for each of the parameters was used. The SFRs have been averaged over the last 100 Myr and the 1σ uncertainties in stellar mass, when compared to both mock groups and other independent estimates, are of the order of 0.15 dex (McGee et al. 2011). For the stellar masses probed in this work [$\log_{10}(M_{\text{star}}/M_{\odot}) \geq 10$], there is no systematic offset between the Bruzual & Charlot (2003) (used for SDSS and GEEC) and Bruzual (2007) (used for GEEC2) models.

Table 1. Properties of the group catalogues.

| Catalogue | Redshift range | # of groups | Photometry |
|--------------------------|------------------|-------------|--|
| SDSS ($r < 17.77$) | $z < 0.1$ | 100 | FUV, NUV, u, g, r, i, z |
| GEEC ($r < 23$) | $0.1 < z < 0.55$ | 37 | FUV, NUV, u, g, r, i, z, K <i>Spitzer</i> : IRAC and MIPS |
| GEEC2 ($r < 24.75$) | $0.8 < z < 1$ | 8 | FUV, NUV, $U, B, V, G,$ R, I, Z, J, K <i>Spitzer</i> : IRAC and MIPS |

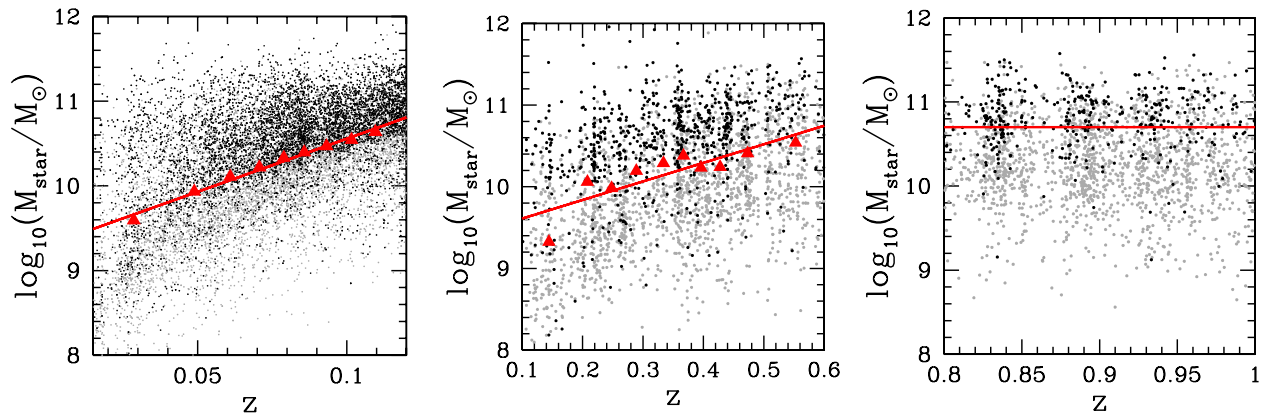


Figure 1. Left-hand panel: observed $\log_{10}(M_{\text{star}}/M_{\odot})$ versus z for the quiescent galaxies (black circles) and for all galaxies (grey circles) in a subsample of 15 000 randomly selected galaxies in the SDSS catalogue. The red triangles indicate the 90th percentile value of the stellar mass estimates of quiescent galaxies (black circles) given by equation (1) within a given redshift bin and the red solid line indicates a linear least-squares fit to these points. This line is taken to be the stellar mass completeness limit of the sample. Middle panel: same as the left-hand panel except for all galaxies in the GEEC sample. Right-hand panel: same as the left-hand panel except for all galaxies in the GEEC2 sample and the red solid line indicates a stellar mass cut of $\log_{10}(M_{\text{star}}/M_{\odot}) = 10.7$.

The observed scatter between the two models is within our quoted 1σ uncertainties. Additionally, there may be additional systematic uncertainties due to, for example, the IMF assumed in the fitting procedure.

2.5 Completeness corrections

The ability to detect faint and low-mass galaxies declines with increasing redshift, which can be seen in Fig. 1 where we plot $\log_{10}(M_{\text{star}}/M_{\odot})$ versus z for all galaxies in each of the catalogues. In order to address this stellar mass incompleteness, we apply a stellar mass limit to each of the group catalogues using the methodology described in Connelly et al. (2012). Briefly, we compute the stellar mass that each galaxy would have if it were observed at the r -band magnitude limit (r_{lim}) of the sample using

$$M_{\text{star},r_{\text{lim}}}(z) = M_{\text{star}}(z) \times 10^{[-0.4[r_{\text{lim}} - r(z)]]}, \quad (1)$$

where $M_{\text{star}}(z)$ is the stellar mass of the galaxy determined from the SED fits and $r(z)$ is the observed r -band magnitude of the galaxy.

We define a conservative stellar mass limit by only taking the passive galaxies with $\text{SSFR} < 10^{-11} \text{ yr}^{-1}$.¹ Since passive galaxies have on average a higher mass-to-light ratio than actively star forming galaxies, we obtain a higher, and therefore more conservative, stellar mass limit using this methodology. To define our limit, we compute the 90th percentile values of the mass estimates (equation 1) for all passive galaxies in narrow redshift bins and then perform a linear least-squares fit to these values. For the SDSS and GEEC catalogues, we then take all galaxies that fall above this line as our stellar mass complete catalogue. To define our stellar mass completeness limit for the high-redshift sample, we take a different approach and apply a cut based on the GEEC2 sample selection criteria and the shape of the stellar mass function of the observed passive galaxy population (Mok et al. 2013). For groups at the high-redshift end ($z \sim 1$) of the GEEC2 catalogue, Mok et al. (2013) found that the sample was complete down to $\log_{10}(M_{\text{star}}/M_{\odot}) = 10.7$ for passive galaxies. We therefore take this value to be our stellar mass limit for the entire

GEEC2 sample. Although a limit of $\log_{10}(M_{\text{star}}/M_{\odot}) = 10.7$ is conservative, we probe galaxy evolution via the quiescent fraction (see Section 2.7), which requires that the population of passive galaxies is complete.

In Fig. 1, we plot the observed stellar masses versus redshift for passive galaxies (black circles) and all galaxies (grey circles) in the SDSS (left-hand panel), GEEC (middle panel) and GEEC2 (right-hand panel) surveys. The 90th percentile stellar mass estimates for the SDSS and GEEC samples are shown as red triangles in Fig. 1 and the linear least-squares fit to these values as the red solid line. For the GEEC2 sample (Fig. 1: right-hand panel), the red solid line indicates our stellar mass limit of $\log_{10}(M_{\text{star}}/M_{\odot}) = 10.7$. The stellar mass ranges for our complete samples are: $9.5 \lesssim \log_{10}(M_{\text{star}}/M_{\odot}) \lesssim 11.5$ for SDSS, $9.6 \lesssim \log_{10}(M_{\text{star}}/M_{\odot}) \lesssim 11.5$ for GEEC and $10.7 \leq \log_{10}(M_{\text{star}}/M_{\odot}) \lesssim 11.5$ for GEEC2.

In addition, we have applied a spectroscopic completeness correction by calculating magnitude weights for each galaxy. The weights are computed following a methodology similar to Wilman et al. (2005b), where weights are calculated in r -band magnitude bins down to the limiting magnitude of each catalogue.

2.6 Final group membership

To probe the effects of group dynamics on the properties of member galaxies, we only consider the sample of group galaxies with measured stellar masses and SFRs. In addition, we only look at groups with more than five member galaxies within two virial radii (r_{200}) of the group centroid, where r_{200} is defined as (Carlberg et al. 1997)

$$r_{200} = \frac{\sqrt{3}\sigma_{\text{rest}}}{10H(z)}, \quad (2)$$

where σ_{rest} is the observed velocity dispersion (σ_{obs}), computed via the Gapper Estimator (Beers, Flynn & Gebhardt 1990) from all member galaxies within 1.0 Mpc of the group centroid, corrected for redshift [i.e. $\sigma_{\text{rest}} = \sigma_{\text{obs}}/(1+z)$] and $H(z) = H_0 \sqrt{\Omega_{\text{m},0}(1+z)^3 + \Omega_{\Lambda,0}}$.

The inclusion of galaxies out to $2r_{200}$ is motivated by previous results. In Hou et al. (2012), we found that substructure galaxies were preferentially located in the group outskirts, beyond the virial radius. Therefore, in order to better study correlations between the amount of substructure and galaxy properties, we include galaxies

¹ It should be noted that Connelly et al. (2012) use red galaxies to define their limits.

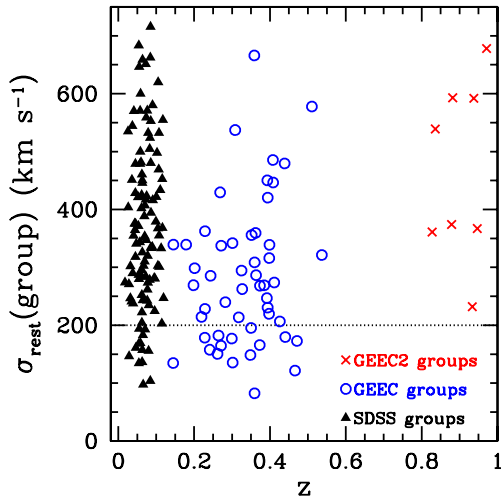


Figure 2. Group velocity dispersion (σ_{rest}) versus redshift (z) for our subsample of groups with $n_{\text{members}} \geq 5$ within $2r_{200}$ of the group centroid identified in SDSS (black triangles), GEEC (blue circles) and GEEC2 (red crosses). The dashed line indicates the lower limit σ_{rest} cut; we only analyse groups with $\sigma_{\text{rest}} > 200 \text{ km s}^{-1}$.

out to $2r_{200}$. We discuss the effects of applying different radial cuts in Section 4.2.

In Fig. 2 we plot the group velocity dispersion (σ_{rest}) versus redshift (z) for our subsample of the three group catalogues. The SDSS, GEEC and GEEC2 groups span a wide range of velocity dispersions, and therefore masses. From Fig. 2, we see that both the SDSS and GEEC group catalogues contain lower mass systems when compared to GEEC2; therefore, to ensure that all three catalogues span a similar mass range, we only consider groups with $\sigma_{\text{rest}} > 200 \text{ km s}^{-1}$, which corresponds to a dynamical mass of $\sim 1.2 \times 10^{13} M_{\odot}$ at a redshift of $z = 0.25$. The minimum of five members within the $2r_{200}$ requirement, and the $\sigma_{\text{rest}} > 200 \text{ km s}^{-1}$ cut, leaves us with 100 SDSS groups, 37 GEEC groups and 8 GEEC2 groups (see Table 1).

2.7 Characterizing the properties of galaxies

In order to study the relationship between environment and galaxy evolution, we look at the SSFRs of the galaxies in groups. We examine both the SSFR distributions and the fraction of quiescent galaxies (hereafter f_q), where f_q is defined as

$$f_q = \frac{\# \text{ galaxies with SSFR} < 10^{-11} \text{ yr}^{-1}}{\text{total \# of galaxies}}, \quad (3)$$

with $\text{SSFR} = 10^{-11} \text{ yr}^{-1}$ marking the division between the main sequence of star-forming galaxies from the quiescent galaxies in the SSFR–stellar mass plane (McGee et al. 2011). It should also be noted that values in equation (3) are weighted to account for spectroscopic incompleteness.

3 GALAXY PROPERTIES WITH GALAXY STELLAR MASS AND GROUP DYNAMICAL MASS

3.1 Correlations with galaxy stellar mass

It is well known that the observed properties of galaxies correlate well with galaxy stellar mass. Many studies have shown that there

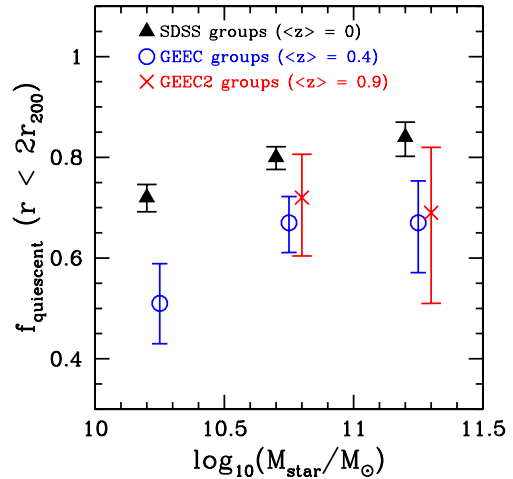


Figure 3. Quiescent fraction (f_q) versus stellar mass for all group galaxies in SDSS (black triangles), GEEC (blue circles) and GEEC2 (red crosses). The data are divided into stellar mass bins of 0.5 dex in the range of $10 \leq \log_{10}(M_{\text{star}}/M_{\odot}) \leq 11.5$ and plotted at the centre of the mass range with small horizontal offsets for clarity. It should be noted that due to our stellar mass cuts, the intermediate-mass galaxies in the GEEC2 sample span a stellar mass range of $10.7 \leq \log_{10}(M_{\text{star}}/M_{\odot}) < 11$. Also, note that all catalogues are stellar mass complete and have been corrected for spectroscopic incompleteness. The uncertainties in the quiescent fraction are computed following the methodology of Cameron (2011).

exists an SFR–stellar mass trend, which is especially strong for star-forming galaxies (Kennicutt 1983; Brinchmann et al. 2004; Noeske et al. 2007; Whitaker et al. 2012), and a colour–stellar mass trend (Tortora et al. 2010; Giodini et al. 2012), where massive galaxies are typically redder and have lower SFRs. Before we investigate the role of group dynamics in galaxy evolution, we must first characterize the stellar mass trend in our sample.

We look at the SSFR–stellar mass trend in each of our three group catalogues. In Fig. 3 we plot f_q (equation 3) versus stellar mass for all galaxy group members in SDSS (black triangles), GEEC (blue circles) and GEEC2 (red crosses). From Fig. 3, we see that the quiescent fraction shows a positive correlation with stellar mass for the SDSS and GEEC samples, as previously noted by McGee et al. (2011). For all three catalogues, the f_q –stellar mass trend appears to be flat for galaxies with $\log_{10}(M_{\text{star}}/M_{\odot}) > 10.5$.

An additional trend that can be seen in Fig. 3 is that for low-mass galaxies [$\log_{10}(M_{\text{star}}/M_{\odot}) < 10.5$] we observe an evolution in the quiescent fraction with redshift, where galaxies at higher redshifts have lower f_q . We see a similar, though less drastic, trend for the massive galaxies [$\log_{10}(M_{\text{star}}/M_{\odot}) > 10.5$] when comparing our $z \sim 0$ and $z \sim 0.4$ samples. However, we do not observe a clear evolution in the quiescent fractions of massive galaxies between $z \sim 0.4$ and $z \sim 0.9$.

In Section 4.2.2, we discuss how we remove this strong correlation between quiescent fraction and stellar mass so that we can examine the effects of group dynamics.

3.2 Correlations with group dynamical mass (M_{200})

There are a number of possible processes related to environmentally driven galaxy evolution, including: ram-pressure stripping, strangulation and galaxy–galaxy interactions. Some of these mechanisms are more directly related to the potential of the group, while others are better correlated to the local or neighbouring environment.

To probe the influence of the host group, we look for correlations between the observed quiescent fraction and dynamical mass, M_{200} , of the group defined as (Carlberg et al. 1997)

$$M_{200} = \frac{3r_{200}\sigma_{\text{rest}}^2}{G}, \quad (4)$$

where r_{200} is given by equation (2). It should be noted that the mass computed in equation (4) assumes that the system is in dynamical equilibrium, which we show in Section 4 is not always true for the groups in our catalogues. Bird (1995) showed that dynamical mass estimators, such as equation (4), tend to overestimate the true mass of systems not in equilibrium, in particular those with significant substructure. However, our goal is to roughly divide our sample by mass and this methodology works well for this purpose. Alternatively, we could have used the total stellar mass of the group to characterize the host environment, though this method requires significant completeness corrections. It should be noted that we do observe similar results whether M_{200} or the total stellar mass is used in the analysis.

We make a cut at $M_{200} = 6 \times 10^{13} M_{\odot}$ to distinguish between low- and high-mass groups as this is the approximate median value for each of the three group catalogues. In Fig. 4, we plot f_q versus z for low-mass galaxies [$10 < \log_{10}(M_{\text{star}}/M_{\odot}) \leq 10.5$: top left-hand panel], intermediate-mass galaxies [$10.5 < \log_{10}(M_{\text{star}}/M_{\odot}) \leq 11$: top right-hand panel]

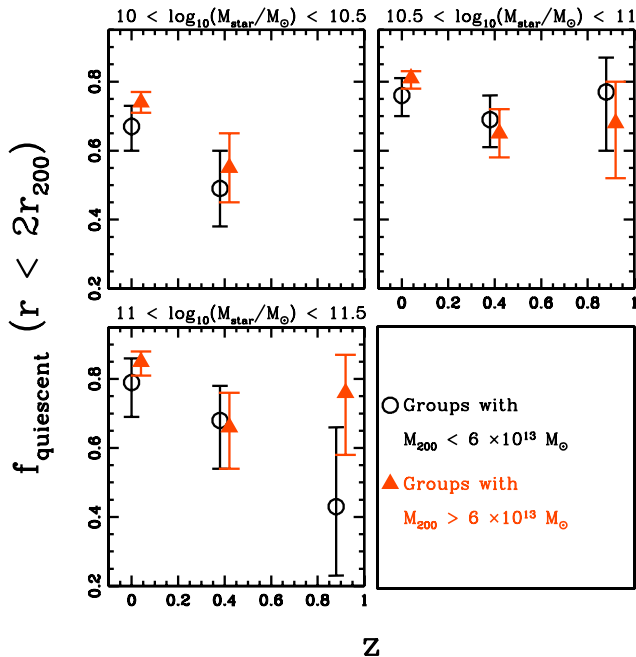


Figure 4. f_q versus z for low-mass galaxies [$10 < \log_{10}(M_{\text{star}}/M_{\odot}) \leq 10.5$: top left-hand panel], intermediate-mass galaxies [$10.5 < \log_{10}(M_{\text{star}}/M_{\odot}) \leq 11$: top right-hand panel] and high-mass galaxies [$11 < \log_{10}(M_{\text{star}}/M_{\odot}) \leq 11.5$: bottom left-hand panel] in low-mass ($M_{200} < 6 \times 10^{13} M_{\odot}$) groups (black circles) and in high-mass ($M_{200} > 6 \times 10^{13} M_{\odot}$) groups (orange triangles). It should be noted that due to our stellar mass cuts, the intermediate-mass galaxies in the GEEC2 sample span a stellar mass range of $10.7 \leq \log_{10}(M_{\text{star}}/M_{\odot}) < 11$. We plot the data at the redshift each sample has been k -corrected to: $z = 0$ for SDSS, $z = 0.4$ for GEEC and $z = 0.9$ for GEEC2, with small horizontal offsets for clarity. We remind the reader of the redshift range for each catalogue: $0 < z < 0.12$ for SDSS, $0.15 < z < 0.55$ for GEEC and $0.8 < z < 1$ for GEEC2. The uncertainties in the quiescent fraction are computed following the methodology of Cameron (2011).

and high-mass galaxies [$11 < \log_{10}(M_{\text{star}}/M_{\odot}) \leq 11.5$: bottom left-hand panel] in low-mass ($M_{200} < 6 \times 10^{13} M_{\odot}$) groups (black circles) and in high-mass ($M_{200} > 6 \times 10^{13} M_{\odot}$) groups (orange triangles). From Fig. 4, we see that for all stellar masses the quiescent fractions of galaxies in low- and high-mass groups are not statistically distinct. It should be noted that if we make an additional cut at $M_{200} = 10^{14} M_{\odot}$, we still find no dependence of f_q on group halo mass. While numerous studies have found that the observed properties of galaxies do correlate with halo mass (Pasquali et al. 2010; Wetzel, Tinker & Conroy 2012), these studies also show that the trends tend to be flatter for higher mass haloes. In particular, given the dynamical mass range of the SDSS, GEEC and GEEC2 groups [$13 \lesssim \log_{10}(M_{200}/M_{\odot}) \lesssim 14.5$] and our average errors on f_q of $\sim \pm 10$ per cent, the average quiescent fractions and ages shown in Wetzel et al. (2012) and Pasquali et al. (2010) are approximately the same for galaxies in low- and high-mass groups, assuming a cut at $M_{200} = 6 \times 10^{13} M_{\odot}$.

4 GROUP DYNAMICS

Having considered how the observed quiescent fraction of galaxies in groups correlates with galaxy stellar mass and group dynamical mass, M_{200} , we now examine how the dynamical state of a group affects the properties of member galaxies. Previous studies of the local environment have been characterized by the local density (e.g. Poggianti et al. 2008) and by the number of nearest neighbours, typically 3–10 (e.g. Gómez et al. 2003; Patel et al. 2011; Sobral et al. 2011). While these methods are effective in determining the local overdensity of regions within groups, they are not directly related to the dynamical state of a group. With a spectroscopic group catalogue we can directly measure the dynamical state of the group, in terms of both the local environment and the host group halo. In the following section, we describe how we classify the dynamical state of galaxy groups and present our analysis of the SDSS, GEEC and GEEC2 groups.

4.1 Determining the dynamical state of groups

We classify the dynamical state of a group using two methods:

- (i) The shape of the group velocity distribution
- (ii) The amount of substructure

Theoretically, a system in dynamical equilibrium (i.e. relaxed or virialized) should have a Gaussian velocity distribution; thus, deviations from such a distribution would indicate a dynamically complex or unevolved system. In Hou et al. (2009), we showed that we can reliably and robustly identify non-Gaussian velocity distributions for systems with as few as five member galaxies using the Anderson–Darling (AD) goodness-of-fit test. A full description of the AD test, and its application to group-sized systems, is given in Hou et al. (2009). For our analysis, we use the AD statistic to compare the cumulative distribution function (CDF) of the ordered galaxy velocities to a Gaussian distribution using the computing formula given as

$$A^2 = -n - \frac{1}{n} \sum_{i=1}^n (2i - 1) (\ln \Phi(x_i) + \ln(1 - \Phi(x_{n+1-i}))), \quad (5)$$

$$A^{2*} = A^2 \left(1 + \frac{0.75}{n} + \frac{2.25}{n^2} \right), \quad (6)$$

where $\Phi(x_i)$, $x_i \leq x \leq x_{i+1}$, is the CDF of a Gaussian distribution (D'Agostino & Stephens 1986). The probabilities, or p -values, are then computed as

$$p = a \exp(-A^{2*}/b), \quad (7)$$

where $a = 3.678\,9468$ and $b = 0.174\,9916$, and both factors are determined via Monte Carlo methods (Nelson 1998). We then classify groups as dynamically complex if the group velocity distribution is identified as non-Gaussian at the 95 per cent confidence level (p -value < 0.05).

We also examine the amount of substructure present in each group by applying the Dressler–Shectman (DS) test (Dressler & Shectman 1988) to our group samples. Substructure is indicative of the recent accretion of galaxies or smaller groups of galaxies (Lacey & Cole 1993). In Hou et al. (2012), we showed that the DS test, originally developed for richer galaxy clusters, could robustly identify substructure for groups with $n_{\text{members}} \geq 20$. Additionally, we found that the test could be applied to groups with as few as 10 members, but in this case the measured fraction of systems with substructure is underestimated. A detailed description of the test, with respect to group-sized systems, can be found in Pinkney et al. (1996), Zabludoff & Mulchaey (1998b) and Hou et al. (2012). Briefly, for each group we compute the mean velocity (\bar{v}) and group velocity dispersion (σ). Then, for each member galaxy i , we compute the local mean velocity (\bar{v}_{local}^i) and local velocity dispersion (σ_{local}^i) using the i th galaxy plus a number of its nearest neighbours (N_{nn}). Using these values, we then compute

$$\delta_i = \left(\frac{N_{\text{nn}} + 1}{\sigma^2} \right) \left[\left(\bar{v}_{\text{local}}^i - \bar{v} \right)^2 + \left(\sigma_{\text{local}}^i - \sigma \right)^2 \right], \quad (8)$$

where $1 \leq i \leq n_{\text{members}}$ and $N_{\text{nn}} = \sqrt{n_{\text{members}}}$, rounded down to the nearest integer. The DS statistic is then computed as

$$\Delta = \sum_{i=1}^n \delta_i. \quad (9)$$

We use Monte Carlo methods to determine the probability or p -value for the DS test, which is done by comparing the observed Δ value to ‘shuffled Δ values’, which are computed by randomly shuffling the observed velocities and then re-assigning them to the observed member galaxy positions. The p -value is then calculated as

$$p = \sum (\Delta_{\text{shuffled}} > \Delta_{\text{observed}}) / n_{\text{shuffle}}, \quad (10)$$

where Δ_{shuffled} and Δ_{observed} are both computed using equation (9). We compute the p -value using 100 000 shuffled Δ values. A group is identified as having significant substructure if it has a p -value < 0.05 .

Following this methodology, we classify the dynamical state of the SDSS, GEEC and GEEC2 groups using the AD test for all groups with $n_{\text{members}} \geq 5$ and the DS test for $n_{\text{members}} \geq 10$. In Table 2, we list the results of the tests, where we find the percentage

Table 2. Fraction of dynamically complex (non-Gaussian) groups and groups with substructure using the AD and DS tests.

| Catalogue | Fraction of non-Gaussian groups | Fraction of groups with substructure |
|-----------|-----------------------------------|--------------------------------------|
| SDSS | 15/100 (15_{-4}^{+6} per cent) | 17/71 (24_{-6}^{+8} per cent) |
| GEEC | 19/37 (51 ± 11 per cent) | 3/14 (21_{-10}^{+19} per cent) |
| GEEC2 | 2/8 (25_{-13}^{+26} per cent) | 1/5 (25_{-12}^{+34} per cent) |

of non-Gaussian groups in the SDSS, GEEC and GEEC2 surveys to be 15_{-4}^{+6} , 51 ± 11 and 25_{-13}^{+26} per cent, while the percentage of groups with detected substructure remains approximately constant at ~ 20 per cent for all three group catalogues.

For completeness, we include the AD and DS test results for the GEE2 sample; however, it should be noted that with such a small sample of systems we cannot robustly determine the fraction of non-Gaussian groups and groups with substructure.

4.2 Dynamics and galaxy properties

Having classified the dynamical state of the groups in our sample, we now compare the SSFR distributions and quiescent fractions of the galaxies in groups that are dynamically young to those in dynamically evolved systems.

4.2.1 SSFR distributions

In the top panels of Fig. 5 we plot the SSFR distributions for galaxies in non-Gaussian (blue dashed line) and Gaussian (solid magenta line) groups identified in the SDSS (left-hand panel), GEEC (middle panel) and GEEC2 (right-hand panel) group catalogues. The bottom panels of Fig. 5 are the same, except we plot the SSFR distributions for galaxies in groups with substructure (blue dashed line) and galaxies in groups with no substructure (solid magenta line) for the SDSS (left-hand panel) and GEEC (middle panel) samples. We do not show the SSFR distributions for the GEEC2 groups with and without substructure because the sample contains too few galaxies. For the same reason we do not include the GEEC2 groups with and without substructure in our analysis for the remainder of the paper.

In all panels of Fig. 5, we see that the histograms are bimodal, showing a population of actively star forming galaxies with $\text{SSFR} > 10^{-11} \text{ yr}^{-1}$ and a population of passive galaxies with $\text{SSFR} < 10^{-11} \text{ yr}^{-1}$. For the SDSS groups, it appears that the SSFR distributions for dynamically complex and relaxed systems, classified with both the AD and DS tests, are similar with a well-populated passive sequence. However, a two-sample Kolmogorov–Smirnov (KS) test indicates that while the SSFR distributions for the SDSS galaxies in groups with and without substructure likely come from the same parent distribution, the distributions for galaxies in Gaussian and non-Gaussian groups are in fact distinct at the ~ 99 per cent confidence level (Table 3). Though it should be noted that the difference is small and it is easier to detect small differences, given the large size of the SDSS sample.

Looking at the $z \sim 0.4$ GEEC groups (middle panels of Fig. 5), we see that the SSFR distributions for the dynamically complex and relaxed groups, identified with either the AD or DS test, look distinct. Indeed, a two-sample KS test indicates that both sets of SSFR distributions come from different parent distributions at a confidence level of > 99 per cent (Table 3). For the Gaussian and non-Gaussian groups, we see that although both histograms show a bimodal distribution with a well-populated passive sequence, there are more galaxies with high SSFRs ($\sim 10^{-10} \text{ yr}^{-1}$; Fig. 5) in the non-Gaussian GEEC groups. The GEEC groups with no detected substructure show a well-populated passive sequence, while the majority of galaxies in the GEEC groups with substructure appear to lie in the actively star forming sequence. A similar result was shown in Hou et al. (2012), where we found that galaxies in groups with substructure had a significantly higher fraction of blue galaxies.

The SSFR distributions for the galaxies in Gaussian and non-Gaussian GEEC2 groups are consistent with coming from the same parent distribution (Table 3) and show similar features to the SDSS

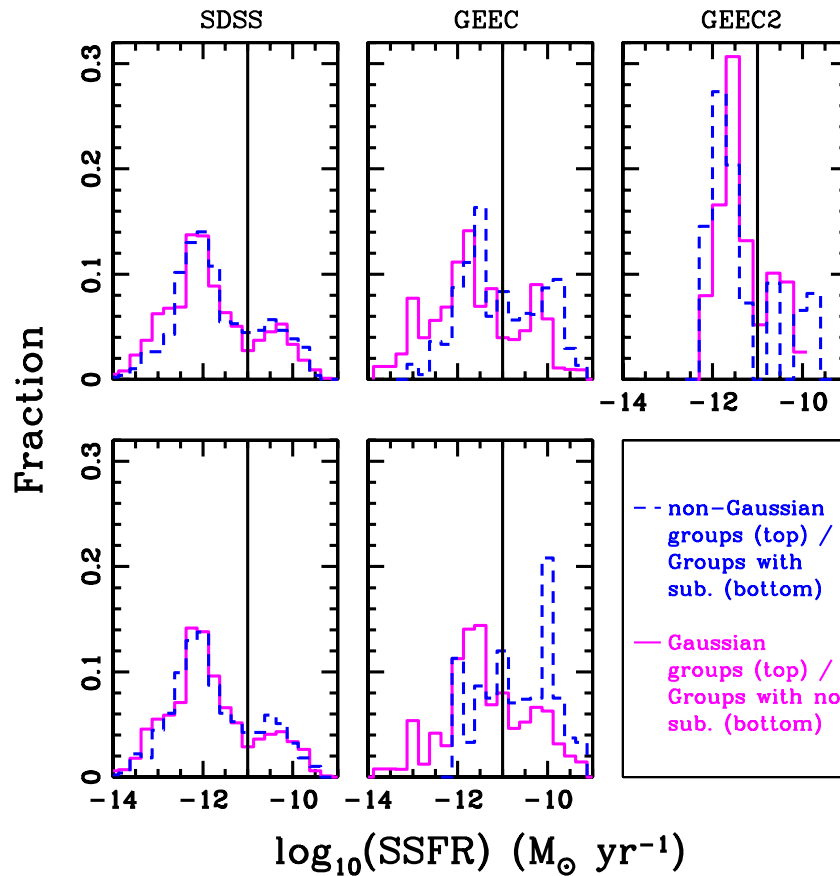


Figure 5. Top panels: SSFR distributions for galaxies in non-Gaussian groups (blue dashed line) and for galaxies in Gaussian groups (magenta solid line) in the SDSS catalogue (left-hand panel), GEEC catalogue (middle panel) and GEEC2 catalogue (right-hand panel). Note that all catalogues are stellar mass complete and spectroscopic completeness weights have been taken into account. Bottom panels: SSFR distributions for galaxies in groups with substructure (blue dashed line) and for galaxies in groups with no identified substructure (magenta solid line) for the SDSS (left-hand panel) and GEEC (middle panel) samples. We do not show the SSFR distributions for the GEEC2 groups with and without substructure, as our stellar mass limit and $n \geq 10$ within the $2r_{200}$ cut for the DS test result in too few galaxies.

Table 3. Probabilities (p -values) from a two-sample KS test comparing the SSFR distributions shown in Fig. 5. Probabilities < 0.01 indicate that the systems come from different underlying parent distributions.

| Catalogue | p -value comparing Gaussian versus non-Gaussian groups | p -value comparing groups with substructure versus no substructure |
|-----------|--|--|
| SDSS | 0.010 99 | 0.4729 |
| GEEC | ~ 0 | ~ 0 |
| GEEC2 | 0.6869 | |

groups (i.e. a dominant quiescent population). The high fraction of quiescent galaxies is likely a result of our stellar mass completeness limits [$\log_{10}(M_{\text{star}}/M_{\odot}) \geq 10.7$], which from Fig. 3 would result in a more dominant quiescent population.

4.2.2 Quiescent fractions

We now look at the quiescent fraction (f_q ; equation 3) of galaxies in dynamically complex and relaxed groups. In the left-hand side of Fig. 6, we plot f_q versus z for low-mass galaxies [$10 < \log_{10}(M_{\text{star}}/M_{\odot}) \leq 10.5$: top left-hand panel], intermediate-mass galaxies [$10.5 < \log_{10}(M_{\text{star}}/M_{\odot}) \leq 11$: top right-hand panel] and high-mass galaxies [$11 < \log_{10}(M_{\text{star}}/M_{\odot}) \leq 11.5$: bottom left-hand panel] in non-Gaussian groups (blue symbols) and in Gaussian

groups (magenta triangles). The panels on the right-hand side are similar, except we plot galaxies in groups with substructure (blue symbols) and in groups with no significant substructure (magenta triangles) but only for the SDSS and GEEC groups. The GEEC2 groups are omitted as there are too few galaxies for a robust substructure analysis. In order to isolate the effects of dynamical state on the properties of galaxies from the strong f_q -stellar mass trend (Fig. 3), we bin our data into narrow bins of stellar mass.

Looking at Fig. 6, we find that at almost all epochs and stellar masses there is no significant difference in the quiescent fractions of galaxies in dynamically complex and relaxed groups for both dynamical classification schemes (AD and DS tests). However, we do observe a difference in the low-mass bin [$10 < \log_{10}(M_{\text{star}}/M_{\odot}) \leq 10.5$] of the GEEC sample, where the

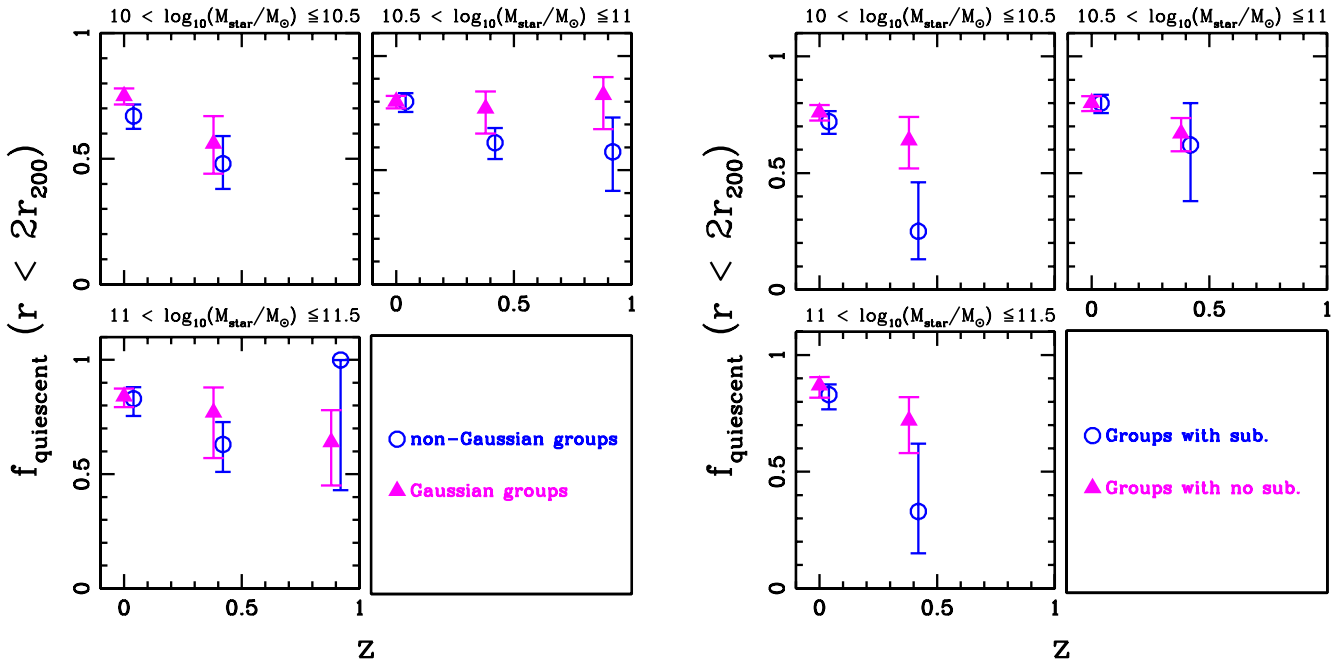


Figure 6. Left-hand side: f_q versus z for galaxies in groups with non-Gaussian velocity distributions (blue circles) and in groups with Gaussian velocity distributions (magenta triangles). The panels are divided into bins of stellar mass: $10 < \log_{10}(M_{\text{star}}/M_{\odot}) \leq 10.5$ (top left-hand panel), $10.5 < \log_{10}(M_{\text{star}}/M_{\odot}) \leq 11$ (top right-hand panel) and $11 < \log_{10}(M_{\text{star}}/M_{\odot}) \leq 11.5$ (bottom left-hand panel). Note that all catalogues are spectroscopic and stellar mass complete. Also, due to the stellar mass limits the intermediate-mass bin for the GEEC2 sample does not extend down to $\log_{10}(M_{\text{star}}/M_{\odot}) \leq 10.5$, but rather covers a range of $10.7 \leq \log_{10}(M_{\text{star}}/M_{\odot}) \leq 11$. We plot the data at the redshift that each sample has been k -corrected to: $z = 0$ for SDSS, $z = 0.4$ for GEEC and $z = 0.9$ for GEEC2, with small horizontal offsets for clarity. Right-hand side: same as the left-hand side except for galaxies in groups with substructure (blue circles) and in groups with no significant substructure (magenta triangles). Again, we do not show the GEEC2 groups with and without substructure, as our stellar mass limits and $n \geq 10$ within the $2r_{200}$ cut for the DS test resulted in too few galaxies in each subsample. The uncertainties in quiescent fraction are computed following the methodology of Cameron (2011).

groups with substructure have a lower f_q than observed in the groups with no substructure.

It should also be noted that our analysis was done using galaxies within two virial radii of the group centroid; however, if we use only galaxies with $r < r_{200}$ we find similar results. Although including galaxies beyond the virial radius (r_{200}) inherently means that we are investigating the ‘unvirialized’ regions of our systems, we find that while the fraction of dynamically young systems increases within each sample, the trends with redshift remain the same whether we use r_{200} or $2r_{200}$. In Hou et al. (2012), we determined that substructure galaxies were preferentially found on the group outskirts. Thus, analysing galaxies out to two virial radii allows us to better study substructure in our groups. Additionally, studies have shown that the effects of the environment on galaxies can extend well beyond the virial radius (Feldmann et al. 2010; von der Linden et al. 2010; Bahe et al. 2013).

5 DISCUSSION

In Section 4, we classified the dynamical state of our group sample and then compared the SSFR distributions and quiescent fractions of galaxies in dynamically complex and relaxed groups. We now discuss the implications of our findings.

5.1 The evolution of group dynamics

In a Λ CDM Universe, structure grows hierarchically through mergers and accretion (e.g. Springel et al. 2005). Numerous studies have shown that at a given halo mass the average accretion rate of

dark matter haloes goes as $\dot{M}/M \propto (1+z)^n$, where $n \sim 1.5\text{--}2.5$ (Birnboim, Dekel & Neistein 2007; McBride, Fakhouri & Ma 2009), indicating that the accretion rate increases with redshift. As a reflection of this assembly history, one might expect the fraction of dynamically unevolved systems to increase with redshift for a given mass. Although, additional factors, such as the time since infall or the mass and orbit of the accreted object, should also affect the evolution of the dynamical state. For example, continuous accretion of smaller subhaloes could result in less obvious deviations from a relaxed state in comparison to an instantaneous major merger of larger haloes (Cohn & White 2005). Therefore, observations that are sensitive to different forms of mass assembly may result in different dynamical evolution scenarios. However, based on a statistical study of a large sample of simulated N -body groups and clusters, identified with an FoF algorithm, Cohn & White (2005) found that on average the virial ratio, 2 kinetic energy/potential energy, of all clusters with $M > 10^{14} h^{-1} M_{\odot}$ increased with increasing redshift. Therefore, systems at higher redshifts are more dynamically young or complex than in the local Universe. Assuming that galaxies are a good tracer of the dark matter haloes, it should be possible to detect this predicted increase in dynamically unevolved systems.

In Section 4.1, we found that the fraction of groups with non-Gaussian velocity distributions, classified as dynamically young, increases significantly from ~ 15 per cent at $z \sim 0$ to ~ 51 per cent at $z \sim 0.4$ (Table 2), which is in agreement with the results of Cohn & White (2005) who found that the virial ratio increased with redshift. From $z \sim 0.4$ to $z \sim 0.9$ it appears that the fraction of non-Gaussian groups is consistent with either being flat or decreasing with increasing redshift (Table 2); however, this result is based on a

small sample of eight high- z groups. It is also important to note that the GEEC2 catalogue is different from the SDSS or GEEC samples in that: the groups were selected using a different methodology, all of the GEEC2 groups are X-ray bright while only some of the SDSS and GEEC groups are X-ray bright, and a different stellar mass completeness limit was applied. Thus, the results of the GEEC2 sample may be due to small number statistics or differences in the sample selection. Further investigation of a larger sample of high-redshift groups is required to make any conclusive statements about the evolution of group dynamics from intermediate to high redshifts.

We now look at the evolution of substructure in groups and we find that the fraction of groups with substructure is consistent out to $z \sim 1$. These results appear to be contradictory. However, the AD and DS tests, though both measures of the dynamical state, probe different stages of dynamical complexity (Pinkney et al. 1996) and a one-to-one correspondence between non-Gaussian groups (identified from the AD test) and groups with substructure (identified from the DS test) does not necessarily hold. In Hou et al. (2012) we showed that groups with substructure that is loosely bound or spatially mixed with members of the host group can be difficult to detect. Therefore, groups with non-Gaussian profiles may have substructure that is missed by the DS test. Also, since we studied groups with as few as 10 members, the results of the DS test can only provide a lower limit on the fraction of groups with substructure (Hou et al. 2012), so the true fraction of groups with substructure is likely higher than the values quoted in Table 2.

5.2 The effects of dynamics on galaxy properties

We first look at the quiescent fraction as a function of redshift. From Figs 3 and 6 we see that for groups only the low-mass galaxies [$10 < \log_{10}(M_{\text{star}}/M_{\odot}) \leq 10.5$] clearly exhibit the well-known Butcher–Oemler effect (Butcher & Oemler 1984; Poggianti et al. 1999; Wilman et al. 2005a; Urquhart et al. 2010; McGee et al. 2011; Li et al. 2012), where f_q decreases with increasing redshift. In contrast, the quiescent fraction of intermediate- and high-mass galaxies [$10.5 < \log_{10}(M_{\text{star}}/M_{\odot}) \leq 11.5$] in groups shows a marginal decrease between $z \sim 0$ to $z \sim 0.4$ and no obvious change between $z \sim 0.4$ to $z \sim 0.9$. This result is similar to those of Raichoor & Andreon (2012), who observed no increase in the fraction of high-mass [$\log_{10}(M_{\text{star}}/M_{\odot}) \gtrsim 11.13$] blue galaxies in clusters in the redshift range of $0 < z < 2.2$. Based on our results, we find no clear evidence for the Butcher–Oemler effect in galaxies with $\log_{10}(M_{\text{star}}/M_{\odot}) \gtrsim 10.5$ in groups out to $z \sim 1$. However, we do observe decrease in the fraction of low-mass [$\log_{10}(M_{\text{star}}/M_{\odot}) < 10.5$] quiescent galaxies with increasing redshift.

Finally, we examine the effects of dynamical state. In general, we find that there is no correlation between the dynamical state and quiescent fraction for massive galaxies [$\log_{10}(M_{\text{star}}/M_{\odot}) > 10.5$]; however, there may be a hint of a correlation with the presence of substructure in our lowest mass galaxies [$10 < \log_{10}(M_{\text{star}}/M_{\odot}) \leq 10.5$ – Fig. 6: right-hand side]. In our intermediate-redshift GEEC sample, the groups with substructure have a lower quiescent fraction in comparison to galaxies in groups with no substructure. Our results for the SDSS sample can be compared to the Zurich Environmental Study sample of Carollo et al. (2012) and are in good agreement. Carollo et al. (2012) found that central galaxies and satellites with $\log_{10}(M_{\text{star}}/M_{\odot}) > 10$ in dynamically relaxed and unrelaxed groups, classified via the DS test, have similar observed galaxy properties. However, these authors did find that satellites with $\log_{10}(M_{\text{star}}/M_{\odot}) < 10$ are bluer by ~ 0.1 mag in unrelaxed groups. Our sample does not extend to these low masses,

though we do find a similar result for slightly higher mass galaxies [$10 < \log_{10}(M_{\text{star}}/M_{\odot}) \leq 10.5$] at intermediate redshifts ($z \sim 0.4$), which could indicate possible redshift evolution in the relationship between substructure and quiescent fraction.

In addition, several studies have also found that environmental effects on galaxy properties can only be observed in low-mass galaxies [$\log_{10}(M_{\text{star}}/M_{\odot}) \lesssim 10.5$ – Peng et al. 2010; Sobral et al. 2011]. In particular, Peng et al. (2010) suggest that for low-mass galaxies at $z \gtrsim 0.5$, the main mechanism responsible for star formation quenching is galaxy–galaxy interactions, which should be the dominant process in dynamically unevolved systems with significant substructure. In addition, Blanton & Berlind (2007) found that while the properties of star-forming galaxies were largely independent of the environment, they did observe a correlation between colour and clustering on small scales ($< 300 h^{-1}$ Mpc), which they claim indicated that substructure within groups may play a role in the evolution of galaxies. Similarly, Wilman, Zibetti & Budavári (2010) observed a correlation between the mean colour of blue galaxies and local density, but only on the $\lesssim 1$ Mpc scales, further suggesting that the local, and not global or large-scale, environment may have a more dominant affect on galaxy evolution.

Although we do observe a difference in the quiescent fractions of low-mass galaxies in GEEC groups with and without substructure, we note that this result is based on a small sample of groups (Table 2). A larger sample of intermediate- and high-redshift groups is required to make a more robust statement about whether quenching in low-mass group galaxies is suppressed in the presence of substructure.

6 CONCLUSIONS

We have looked at the role of galaxy stellar mass, group dynamical mass (M_{200}) and dynamical state in the evolution of galaxies in groups out to $z \sim 1$ using the SDSS, GEEC and GEEC2 group catalogues. The dynamical states of the groups are classified with the AD test to distinguish between Gaussian and non-Gaussian velocity distributions and with the DS test to determine the amount of substructure within the groups. The main results of this analysis are as follows:

- (i) We observe a strong trend between the quiescent fraction and galaxy stellar mass in SDSS and GEEC, where higher mass galaxies have higher f_q , similar to the results of McGee et al. (2011).
- (ii) There is no measurable difference in the quiescent fraction of galaxies in low-mass ($10^{13} \lesssim M_{200} < 6 \times 10^{13} M_{\odot}$) and high-mass ($6 \times 10^{13} M_{\odot} < M_{200} \lesssim 10^{14.5} M_{\odot}$) groups at all stellar masses.
- (iii) The fraction of groups with non-Gaussian velocity distributions increases from $z \sim 0$ to $z \sim 0.4$, while the fraction of groups with detected substructure is constant out to $z \sim 1$.
- (iv) We observe the Butcher–Oemler effect in groups, where groups at higher redshifts have lower quiescent fractions, but only for low-mass galaxies [$10 < \log_{10}(M_{\text{star}}/M_{\odot}) \lesssim 10.5$], while galaxies with $\log_{10}(M_{\text{star}}/M_{\odot}) > 10.5$ show little or no evidence of the Butcher–Oemler effect out to $z \sim 1$.
- (v) We do not observe a significant difference in the quiescent fractions of massive galaxies [$\log_{10}(M_{\text{star}}/M_{\odot}) > 10.5$] in dynamically complex and relaxed groups, where the dynamical state is defined either by the AD or by the DS test.
- (vi) We observe a marginally lower quiescent fraction for low-mass galaxies [$10 \leq \log_{10}(M_{\text{star}}/M_{\odot}) < 10.5$] in groups with detected substructure at $z \sim 0.4$ when compared to groups with no significant substructure.

In conclusion, we find that there is no strong correlation between the dynamical state of a group and the observed quiescent fraction for massive galaxies; however, we do see possible signs of a correlation between f_q and substructure at $z \sim 0.4$. This result suggests that environmental effects on galaxy evolution are only evident in low-mass galaxies. In order to better understand the role of group dynamics, and the environment in general, on the evolution of galaxies, it is necessary to probe lower mass galaxies [$\log_{10}(M_{\text{star}}/M_{\odot}) < 10.5$] where these mechanisms likely dominate.

ACKNOWLEDGEMENTS

We would like to thank the CNOC2 team for the use of unpublished redshifts. AH, LCP and WEH would like to thank the National Science and Engineering Research Council of Canada for funding.

REFERENCES

- Abadi M. G., Moore B., Bower R. G., 1999, *MNRAS*, 308, 947
 Adelman-McCarthy J. K. et al., 2008, *ApJS*, 175, 297
 Bahe Y. M., McCarthy I. G., Balogh M. L., Font A. S., 2013, *MNRAS*, 430, 3017
 Baldry I. K., Balogh M. L., Bower R. G., Glazebrook K., Nichol R. C., Bamford S. P., Budavari T., 2006, *MNRAS*, 373, 469
 Balogh M. L., Navarro J. F., Morris S. L., 2000, *ApJ*, 540, 113
 Balogh M. L., Baldry I. K., Nichol R., Miller C., Bower R., Glazebrook K., 2004, *ApJ*, 615, L101
 Balogh M. L. et al., 2007, *MNRAS*, 374, 1169
 Balogh M. L. et al., 2009, *MNRAS*, 398, 754
 Balogh M. L. et al., 2011, *MNRAS*, 412, 2303
 Barnes J., 1985, *MNRAS*, 215, 517
 Beers T. C., Flynn K., Gebhardt K., 1990, *AJ*, 100, 32
 Berlind A. A. et al., 2006, *ApJS*, 167, 1
 Bird C. M., 1995, *ApJ*, 445, L81
 Birnboim Y., Dekel A., Neistein E., 2007, *MNRAS*, 380, 339
 Blanton M. R., Berlind A. A., 2007, *ApJ*, 664, 791
 Blanton M. R. et al., 2003, *ApJ*, 594, 186
 Blanton M. R., Eisenstein D., Hogg D. W., Schlegel D. J., Brinkmann J., 2005, *ApJ*, 629, 143
 Bolzonella M. et al., 2010, *A&A*, 524, A76
 Brinchmann J., Charlot S., White S. D. M., Tremonti C., Kauffmann G., Heckman T., Brinkmann J., 2004, *MNRAS*, 351, 1151
 Brough S., Forbes D. A., Kilborn V. A., Couch W., 2006, *MNRAS*, 370, 1223
 Bruzual G., 2007, in Vallenari A., Tantalò R., Portinari L., Moretti A., eds, *ASP Conf. Ser. Vol. 374, From Stars to Galaxies: Building the Pieces to Build Up the Universe*. Astron. Soc. Pac., San Francisco, p. 303
 Bruzual G., Charlot S., 2003, *MNRAS*, 344, 1000
 Butcher H., Oemler A., Jr, 1984, *ApJ*, 285, 426
 Cameron E., 2011, *PASA*, 28, 128
 Carlberg R. G. et al., 1997, *ApJ*, 485, L13
 Carlberg R. G., Yee H. K. C., Morris S. L., Lin H., Hall P. B., Patton D. R., Sawicki M., Shepherd C. W., 2001, *ApJ*, 552, 427
 Carollo C. M. et al., 2012, preprint (arXiv e-prints)
 Charlot S., Fall S. M., 2000, *ApJ*, 539, 718
 Cohn J. D., White M., 2005, *Astrophys. J.*, 24, 316
 Connelly J. L. et al., 2012, *ApJ*, 756, 139
 Cooper M. C. et al., 2008, *MNRAS*, 383, 1058
 Cox T. J., Jonsson P., Primack J. R., Somerville R. S., 2006, *MNRAS*, 373, 1013
 D'Agostino R., Stephens M., 1986, *Goodness-of-fit Techniques*. Marcel Dekker Inc., New York
 De Lucia G., Fontanot F., Wilman D., Monaco P., 2011, *MNRAS*, 414, 1439
 De Lucia G., Weinmann S., Poggianti B. M., Aragón-Salamanca A., Zaritsky D., 2012, *MNRAS*, 423, 1277
 Dressler A., 1980, *ApJ*, 236, 351
 Dressler A., Shectman S. A., 1988, *AJ*, 95, 985
 Eke V. R., Baugh C. M., Cole S., Frenk C. S., King H. M., Peacock J. A., 2005, *MNRAS*, 362, 1233
 Elbaz D., Cesarsky C. J., 2003, *Sci*, 300, 270
 Feldmann R., Carollo C. M., Mayer L., Renzini A., Lake G., Quinn T., Stinson G. S., Yepes G., 2010, *ApJ*, 709, 218
 Finoguenov A. et al., 2007, *ApJS*, 172, 182
 Finoguenov A. et al., 2009, *ApJ*, 704, 564
 Geller M. J., Huchra J. P., 1983, *ApJS*, 52, 61
 George M. R. et al., 2011, *ApJ*, 742, 125
 Giodini S. et al., 2012, *A&A*, 538, A104
 Gómez P. L. et al., 2003, *ApJ*, 584, 210
 Gunn J. E., Gott J. R., III, 1972, *ApJ*, 176, 1
 Hogg D. W. et al., 2003, *ApJ*, 585, L5
 Hou A., Parker L. C., Harris W. E., Wilman D. J., 2009, *ApJ*, 702, 1199
 Hou A. et al., 2012, *MNRAS*, 421, 3594
 Kauffmann G., White S. D. M., Heckman T. M., Ménard B., Brinchmann J., Charlot S., Tremonti C., Brinkmann J., 2004, *MNRAS*, 353, 713
 Kawata D., Mulchaey J. S., 2008, *ApJ*, 672, L103
 Kennicutt R. C., Jr, 1983, *ApJ*, 272, 54
 Lacey C., Cole S., 1993, *MNRAS*, 262, 627
 Larson R. B., Tinsley B. M., Caldwell C. N., 1980, *ApJ*, 237, 692
 Li I. H., Yee H. K. C., Hsieh B. C., Gladders M., 2012, *ApJ*, 749, 150
 McBride J., Fakhouri O., Ma C.-P., 2009, *MNRAS*, 398, 1858
 McGee S. L., Balogh M. L., Henderson R. D. E., Wilman D. J., Bower R. G., Mulchaey J. S., Oemler A., Jr, 2008, *MNRAS*, 387, 1605
 McGee S. L., Balogh M. L., Bower R. G., Font A. S., McCarthy I. G., 2009, *MNRAS*, 400, 937
 McGee S. L., Balogh M. L., Wilman D. J., Bower R. G., Mulchaey J. S., Parker L. C., Oemler A., 2011, *MNRAS*, 413, 996
 Martin D. C. et al., 2005, *ApJ*, 619, L1
 Mok A. et al., 2013, *MNRAS*, 431, 1090
 Morrissey P. et al., 2007, *ApJS*, 173, 682
 Muzzin A. et al., 2012, *ApJ*, 746, 188
 Nelson L., 1998, *J. Qual. Technol.*, 30, 298
 Noeske K. G. et al., 2007, *ApJ*, 660, L43
 Oemler A., Jr, 1974, *ApJ*, 194, 1
 Pasquali A., Gallazzi A., Fontanot F., van den Bosch F. C., De Lucia G., Mo H. J., Yang X., 2010, *MNRAS*, 407, 937
 Patel S. G., Kelson D. D., Holden B. P., Franx M., Illingworth G. D., 2011, *ApJ*, 735, 53
 Peng Y.-j. et al., 2010, *ApJ*, 721, 193
 Pinkney J., Roettiger K., Burns J. O., Bird C. M., 1996, *ApJS*, 104, 1
 Poggianti B. M., Smail I., Dressler A., Couch W. J., Barger A. J., Butcher H., Ellis R. S., Oemler A., Jr, 1999, *ApJ*, 518, 576
 Poggianti B. M. et al., 2008, *ApJ*, 684, 888
 Raichoor A., Andreon S., 2012, *A&A*, 537, A88
 Salim S. et al., 2007, *ApJS*, 173, 267
 Sanders D. B., Soifer B. T., Elias J. H., Madore B. F., Matthews K., Neugebauer G., Scoville N. Z., 1988, *ApJ*, 325, 74
 Scoville N. et al., 2007, *ApJS*, 172, 38
 Sobral D., Best P. N., Smail I., Geach J. E., Cirasuolo M., Garn T., Dalton G. B., 2011, *MNRAS*, 411, 675
 Springel V. et al., 2005, *Nat*, 435, 629
 Teyssier R., Chapon D., Bournaud F., 2010, *ApJ*, 720, L149
 Tortora C., Napolitano N. R., Cardone V. F., Capaccioli M., Jetzer P., Molinaro R., 2010, *MNRAS*, 407, 144
 Tyler K. D. et al., 2011, *ApJ*, 738, 56
 Urquhart S. A., Willis J. P., Hoekstra H., Pierre M., 2010, *MNRAS*, 406, 368
 von der Linden A., Wild V., Kauffmann G., White S. D. M., Weinmann S., 2010, *MNRAS*, 404, 1231
 Wetzel A. R., Tinker J. L., Conroy C., 2012, *MNRAS*, 424, 232
 Whitaker K. E., van Dokkum P. G., Brammer G., Franx M., 2012, *ApJ*, 754, L29
 Wilman D. J. et al., 2005a, *MNRAS*, 358, 88

Wilman D. J., Balogh M. L., Bower R. G., Mulchaey J. S., Oemler A., Carlberg R. G., Morris S. L., Whitaker R. J., 2005b, MNRAS, 358, 71
Wilman D. J. et al., 2008, in Kodama T., Yamada T., Aoki K., eds, ASP Conf. Ser. Vol. 399, Panoramic Views of Galaxy Formation and Evolution. Astron. Soc. Pac., San Francisco, p. 340
Wilman D. J., Oemler A., Mulchaey J. S., McGee S. L., Balogh M. L., Bower R. G., 2009, ApJ, 692, 298
Wilman D. J., Zibetti S., Budavári T., 2010, MNRAS, 406, 1701

Yang X., Mo H. J., van den Bosch F. C., Pasquali A., Li C., Barden M., 2007, ApJ, 671, 153
Yee H. K. C. et al., 2000, ApJS, 129, 475
Zabludoff A. I., Mulchaey J. S., 1998a, ApJ, 496, L5
Zabludoff A. I., Mulchaey J. S., 1998b, ApJ, 498, 39

This paper has been typeset from a $\text{\TeX}/\text{\LaTeX}$ file prepared by the author.